FR 7901944

INIS

# SCATTERING OF STRONGLY ABSORBED PARTICLES NEAR THE COULOMB BARRIER

**B. Fernandez**

*DPh-N/BE, CEN Saclay, BP 2, 91190 Gif-sur-Yvette, France*

International discussion meeting "Wath do we know about radical shape of nuclei in the Ca region ?".
Karlsruhe, Germany FR, May 2 - 4, 1979
CEA - CONF 4674

## I. Introduction

What can we learn from the elastic scattering of strongly absorbed particles near the Coulomb barrier? If we define a strongly absorbed particle as a particle which is totally absorbed once it has surmounted the Coulomb barrier, we see immediately that we are going to learn something on the tail of the potential outside of the Coulomb barrier, which is in turn influenced by the tail of the density distributions of the colliding nuclei. In the present talk I will show in part II what can be deduced from α-scattering near the barrier on a large range of nuclei, *not including* calcium region, and in part III what can be deduced from $^{16}O$ scattering near the Coulomb barrier on some calcium isotopes.

## II. Elastic scattering of α particles from medium and heavy nuclei

Figs. 1 and 2 show two examples of α-particle scattering near the Coulomb barrier on medium and heavy nuclei. Fig. 1 shows excitation functions which were measured near 180° at the Saclay tandem by Badawy et al.[1] from a range of nuclei from $^{110}Cd$ to $^{208}Pb$. Fig. 2 shows an angular distribution measured at 22 MeV from $^{209}Bi$ by Barnett and Lilley [2]. Both types of data can be interpreted in the framework of a four-parameter optical model with strong absorption, and very good fits are obtained (the lines in Figs. 1 and 2 are optical model fits).

The signature of strong absorption is not as simple as it is at higher energies, where the reflection coefficients $|\eta_\ell|$ jump from zero to one in a few $\ell$-values near the grazing angular momentum. Here, the angular momenta involved are small and their effective barriers are close to each other. As a result, $\eta_\ell$ varies smoothly from small values to one as a function of $\ell$. Strong absorption is characterized by the fact that the calculated cross-sections are insensitive to the depth of the imaginary potential inside the Coulomb barrier, provided it has some minimum value which insures the total absorption of particles. This is apparent in Fig. 3, where the $\chi^2$ is plotted as a function of W (all other parameters being kept fixed). Clearly any value between 10 and about 50 MeV will give almost the same fit to the data. Another indication is the agreement with incoming wave boundary (IWB) calculations which *assume* strong absorption from the beginning [3]. However, D.F. Jackson and M. Rhoades-Brown [4] have shown that strong absorption is not necessary to fit the data. Equally good fits are obtained with weakly absorbing potentials. The signature of weak absorption is here an odd-even staggering of $|\eta_\ell|$ as a function of $\ell$, as compared to their smooth behaviour in the case of strong absorption. Fig. 4 from ref.[4]. shows the reflection coefficients for different real potentials, and with a (weakly

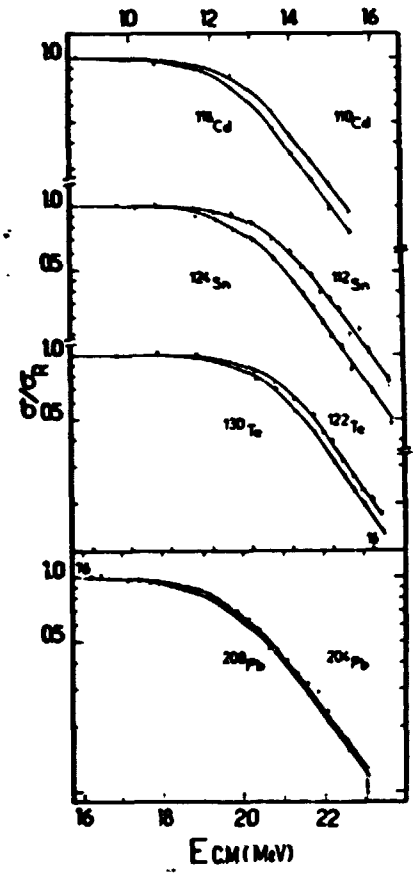


*Figure 1*

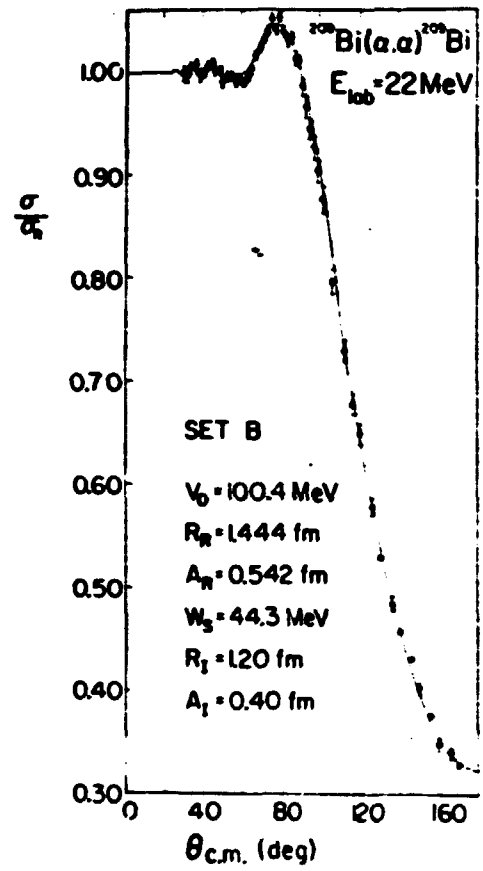


*Figure 2*

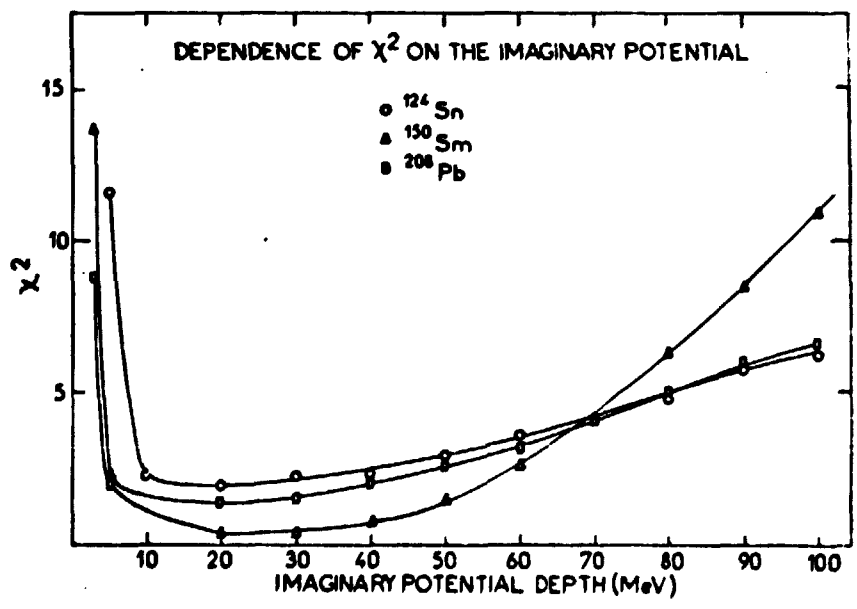


*Figure 3*

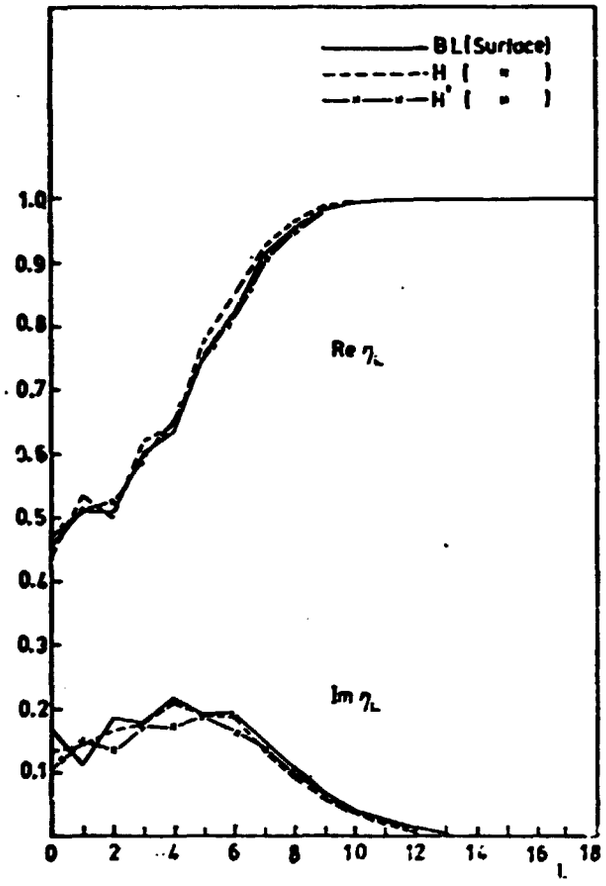


*Figure 4*

a $^{288}$Pb nucleus has very little chances of not being absorbed and form $^{210}$Po, which can certainly offer all possible phase space at 19 MeV excitation. That was in any case the attitude we adopted to analyse the Saclay data [1] and I will discuss now which conclusions can be arrived at if strong absorption is assumed.

In a strong absorption situation, the data are only sensitive to the real potential outside of the Coulomb barrier. As a consequence, only two parameters at best can be determined namely the Igo constant V exp $\frac{R}{a}$ and the diffuseness parameter a. However, at energies close to the Coulomb barrier, absorbing) surface imaginary potential which was ajusted to give the best fit to the Pb(α,α) data of Barnett and Lilley [2] at 22 MeV. Fig. 5 shows the $\eta_\ell$'s obtained by Barnett and Lilley for either volume (strong) absorption (full line) or surface (weak) absorption (dashed line). The calculated cross-sections are essentially identical except at small angles where the latter gives more interferences, but even there differences are on the 1 % level. In the absence of a small-angle, very precise experiment, it is largely a matter of taste to decide if there is weak or strong absorption. My personal prejudice is that an α particle which penetrates

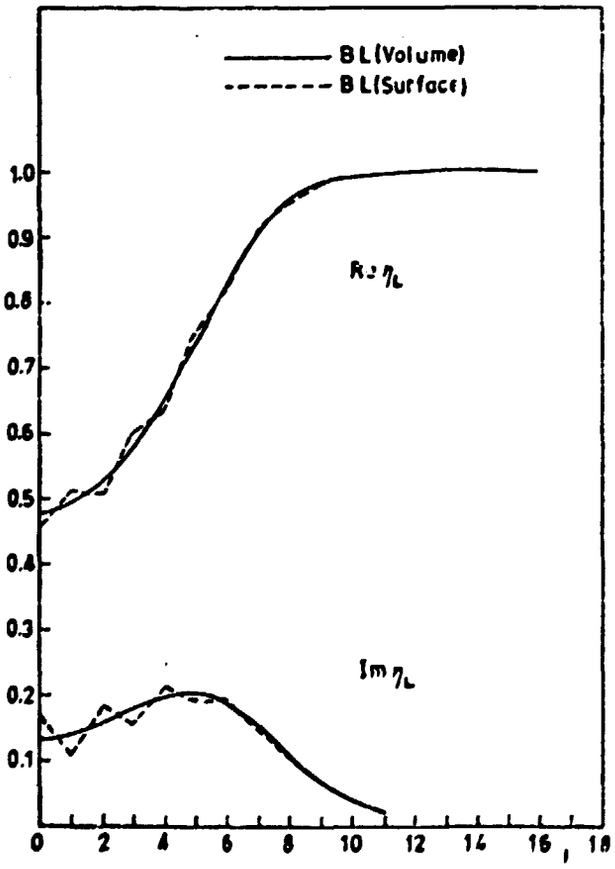


*Figure 5*

the data are very insensitive to the value of $\underline{a}$ and only one size parameter can be determined. Goldring et al.[5] have used the α-nucleus distance at the maximum of the Coulomb barrier, which they call the Rutherford radius $r_R$, while Tabor et al.[3] have used a "constant fraction" radius where the ratio of the nuclear and Coulomb potentials is 2 %. In the analysis of the Saclay data, we found that all potentials giving a good fit cross in a very narrow region, where their depth is about 0.2 MeV, see Fig. 6. Therefore the best choice for a size parameter is the α-nucleus distance $R_{0.2}$ such as $V(R_{0.2}) = -0.2$ MeV. In other words, all parameters $V_o$, $R_{opt}$, and $\underline{a}$ which give a good fit obey the relationship

$$V_o \exp\frac{R_{opt} - R_{0.2}}{a} = -0.2 \text{ MeV} \qquad (1)$$

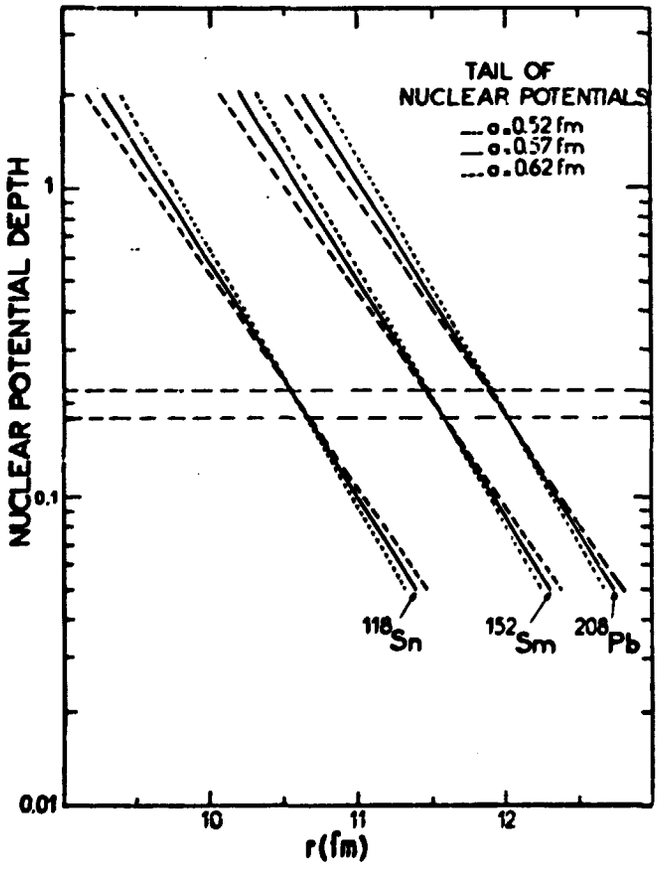


*Figure 6*

What does that imply on the density distribution of the target nucleus? Barnett and Lilley [2] have analysed their $^{209}$Bi data by folding an effective force of Woods-Waxon type into various density distributions of Fermi shape and found that all densities which gave a good fit to the data crossed in a narrow region near $2 \times 10^{-3}$ nucleon/fm$^3$. They used the effective α-nucleon interaction deduced from p-α and n-α free scattering at low energy by Mailandt et al.[6], namely at the barrier

$$V_{eff}(r) = 42.5 \left[1 + \exp\frac{r-2.27}{0.34}\right]^{-1}$$

(MeV, r in fm) (2)

The Saclay data were analysed using a variety of forces and density shapes, in order to determine which was the best determined density region and to which extend the result would depend on such choices. It was found that the choice of the shape of the distribution was not crucial. Either a simple Fermi shape

$$\rho(r) = \frac{\rho_o}{1 + \exp \frac{r - c_N}{a_N}} \qquad (F2)$$

or a "modified gaussian" shape [7]

$$\rho(r) = \rho_o \frac{1 + W \left(\frac{r}{c_N}\right)^2}{1 + \exp \frac{r^2 - c_N^2}{a_N^2}} \qquad (MG)$$

gave similar results.

In contrast, the results are more sensitive to the range of the effective force used. Four such forces have been used, either of gaussian shape

$$V_{eff}(r) = U_o \exp(- K^2 r^2)$$

or of Woods-Saxon shape

$$V_{eff}(r) = \frac{U_o}{1 + \exp \frac{r - R_{eff}}{a_{eff}}},$$

namely

(1) Gaussian, with $U_o = -127$ MeV and $K = 0.6$ fm$^{-1}$ (G1)
(2) Gaussian, with $U_o = -42.5$ MeV and $K = 0.5$ fm$^{-1}$ (G2)
(3) Gaussian, with $U_o = -37$ MeV and $K = 0.5$ fm$^{-1}$ (G3)
(4) Woods-Saxon, with $U_o = -42.5$ MeV, $R_{eff} = 2.35$ fm and $a_{eff} = 0.34$ fm (WS)

The gaussian force G1 or, equivalently, the Woods-Saxon force WS, were found by Sumner [8] to give the best fit to his 42 MeV α scattering on $^{40}$Ca, when he used for the $^{40}$Ca density the Hartree-Fock calculation of Negele [9]. It is quite remarkable that this Woods-Saxon force WS is so close to the one deduced from quite different data by Mailandt et al.[6]. Batty et al.[10] have found that the range of gaussian forces should be between 0.5 and 0.6 fm$^{-1}$, and that $U_o$ and K are then linked by the relationship

$$U_o K^{-6} \simeq 2600 \text{ MeV fm}^6. \qquad (2)$$

The gaussian force G1 and G2 have both

$$U_o K^{-6} = 2720 \text{ MeV fm}^6.$$

Finally, force G3 was derived by Bernstein [11] by folding a nucleon-nucleon force into a density distribution of the α particle. The calculated potentials with WS and G1 are equal within less than 1.5 keV outside of the Coulomb barrier, which makes these forces strictly equivalent.

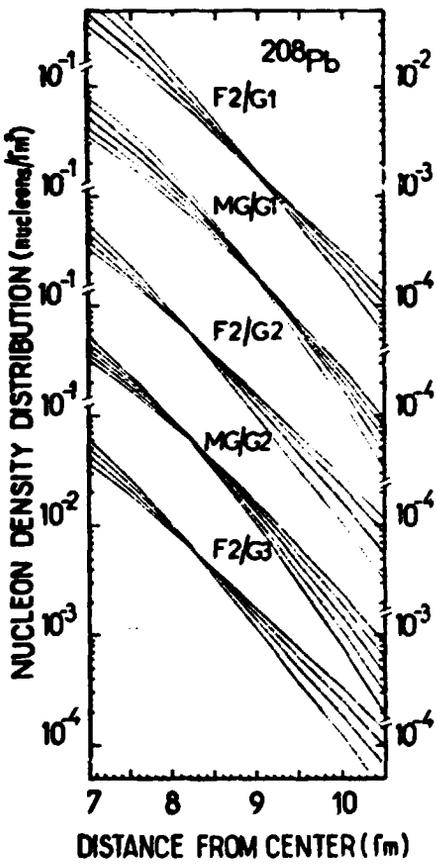


*Figure 7*

The different combinations of density shapes and effective forces which give a good fit to the $^{208}Pb(\alpha,\alpha)$ are represented on Fig. 7. Taking all such combinations into account leads to the determination of the radial distance $r_{0.002}$ where the density is 0.002 nucleon/fm$^3$ with a model-dependent uncertainty of ± 0.14 fm. From tin to lead, there exists a simple relationship between $r_{0.002}$ and the α-nucleus distance $R_{0.2}$ determined in the Woods-Saxon analysis :

$$r_{0.002} = R_{0.2} - (3.11 \pm 0.14)\text{fm}. \qquad (3)$$

If we restrict the values of the range of the force, the model-dependent uncertainty is much smaller. We feel that there are some good evidences in favor of G1 ($K = 0.6$ fm$^{-1}$) :

a) it is essentially identical to WS, which was deduced quite independently,

b) it also gives a good fit to the $^{208}Pb$ data both at 42 MeV and at the barrier when the best calculated densities are used (1).

If we therefore restrict ourselves to G1, we have

$$r_{0.002} = R_{0.2} - (3.06 \pm 0.03)\text{fm}. \qquad (4)$$

The values of $r_{0.002}$ were deduced that way for 23 nuclei from $^{110}Cd$ to $^{208}Pb$. They are shown on Fig. 8. Spherical nuclei follow a line

$$r_{0.002} = 1.355\ A^{1/3} + 0.87\ \text{fm}. \qquad (5)$$

Now, what about the calcium region? Some time ago, we tried a measurement at Saclay on $^{40,42,44,48}Ca$, looking at the elastic scattering near 180° as a function of energy. The results are shown on Fig. 9. It is very clear from this figure that ALAS was also present at the barrier, and in fact on all four calcium isotopes, and consequently no simple optical model analysis could be done

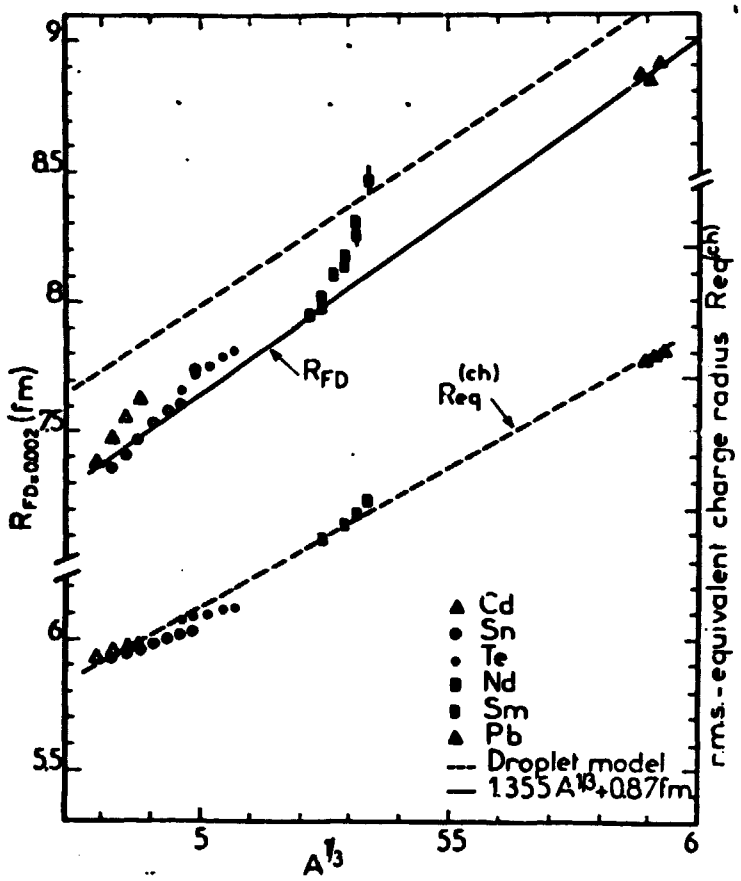


*Figure 8*

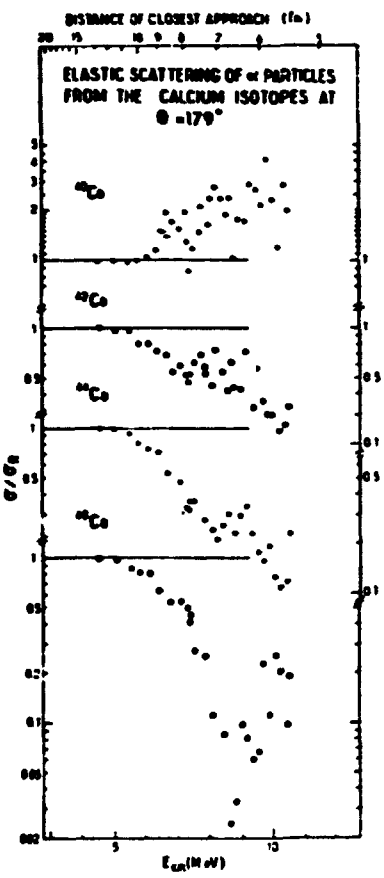


*Figure 9*

to learn something on the density distributions. I will therefore now turn to another projectile which *is* strongly absorbed in collisions with $^{40}$Ca at the barrier, $^{16}$O.

## III. Elastic scattering of $^{16}$O from calcium isotopes

The elastic scattering of $^{16}$O near the Coulomb barrier was first used by Bertin et al.[12] in order to gain some information on the relative sizes of $^{40,44,48}$Ca, after they observed that α scattering, as I said before, proved to be unsuitable for that purpose. They bombarded calcium targets by an oxygen beam between 20 and 42 MeV and observed the elastically scattered ions at lab.angles of 50°, 70°, 90°, 110° and 130°. The Coulomb barrier for $^{40}$Ca is 23.5 MeV (c.m.) or 32.9 MeV (lab). The analysis of these data was made along the lines of ref. [5], in terms of the Rutherford radius deduced from a four-parameter optical model analysis. Fig. 10 shows their measurements for $^{48}$Ca, with optical model fits to $^{48}$Ca and $^{40,44}$Ca as well.

A new measurement of elastic scattering of $^{16}$O was made by Groeneveld et al. [13] on $^{40}$Ca and $^{48}$Ca, with another purpose in mind. They wanted to check a

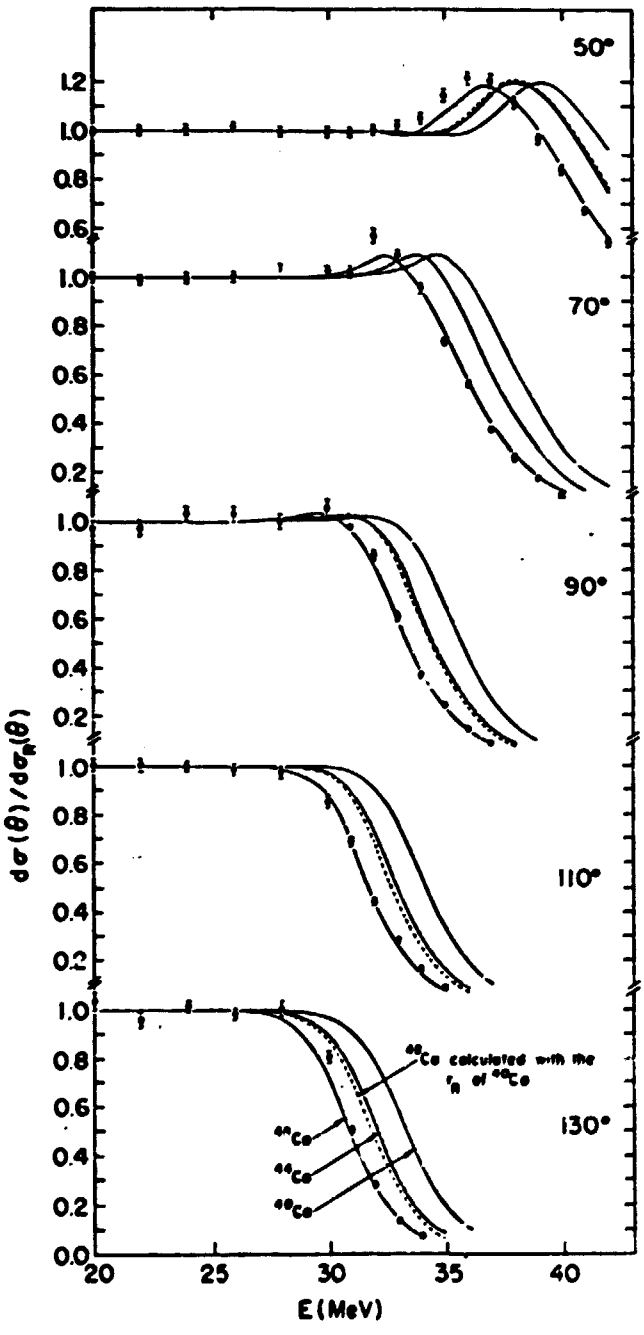


*Figure 10*

prediction made by Chatwin et al. [14] on the occurrence of resonances in the $^{16}O + ^{40}Ca$ elastic scattering, on the basis of the optical model with $\ell$-dependent imaginary potential. Their data comprise excitation functions measured near 180° with an annular detector from 23 to 36 MeV, see Fig. 9, and angular distributions measured at 40 MeV(lab), see Fig. 11. The analysis of these data was made with a conventional four-parameter optical model (the lines in Figs. 11 and 12 are optical model fits) and the Rutherford radius was extracted. These data are very well suited to an analysis in terms of nuclear density distribution, which I have made recently and which I will now discuss.

A first investigation in terms of Woods-Saxon potential shows no sensitivity to the diffuseness parameter a, when it is allowed to vary from 0.5 to 0.7 fm. All potentials that give a good fit to the data lie within the hatched area of Fig. 13 (bottom part). It is clear that the nucleus-nucleus distance at which the potential is about 1 MeV deep is, to a large extent, independent of the choice of parameters V, $R_{opt}$ and $\underline{a}$. We can for example determine for $^{40}Ca$ :

$$R_{1.0} = 9.50 \pm 0.03 \text{ fm}$$

or

$$R_{0.8} = 9.65 \pm 0.02 \text{ fm}.$$

The uncertainties quoted here are only the "model dependent" uncertainty.

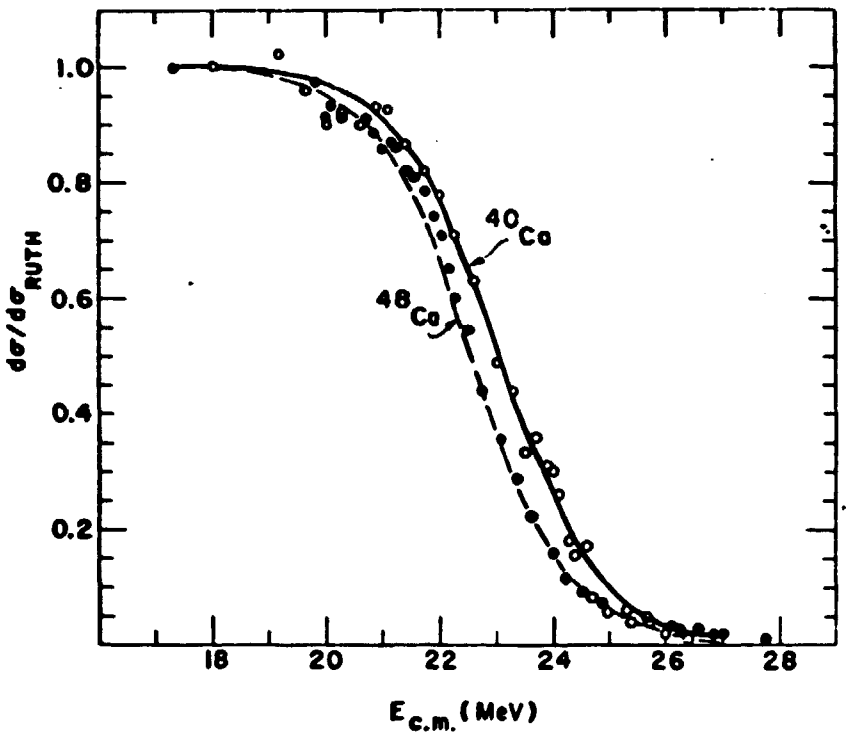


*Figure 11*

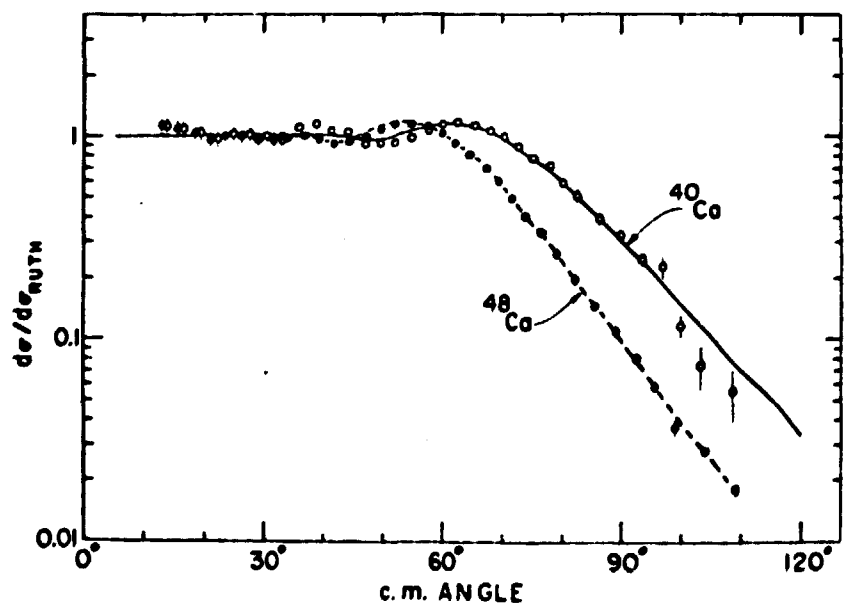


*Figure 12*

Let us now turn to a double folding model analysis. For that purpose I will take the view point that the best Hartree-Fock calculations available to-day for the doubly magic, N = Z, nuclei $^{16}O$ and $^{40}Ca$ give the neutron distribution as exactly as the proton distribution, to which they give very good fits. I have

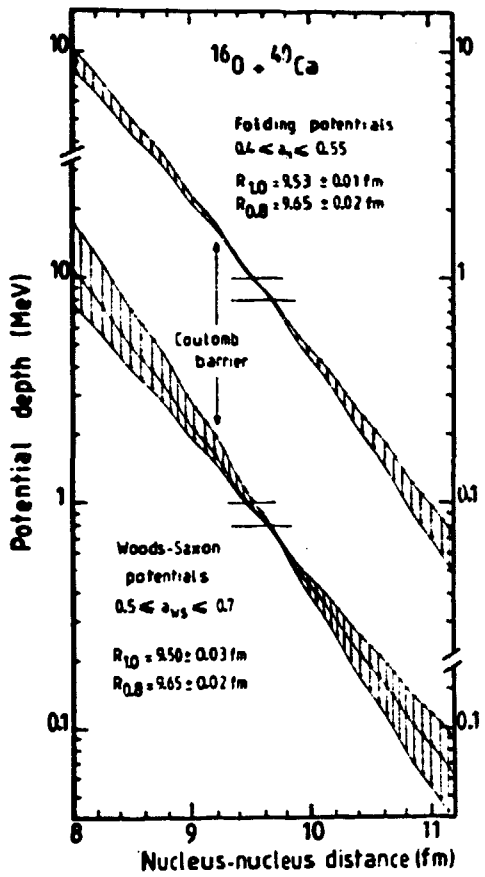


*Figure 13*

used the Hartree-Fock calculations of Campi [15]. It is now necessary to choose an effective nucleon-nucleon force which will generate by folding with these two densities a potential giving a good fit to the data. I have used the interaction of Satchler and Love [16], namely

$$V_{oo}(r) = U_1 \frac{\exp(-\mu_1 r)}{\mu_1 r} + U_2 \frac{\exp(-\mu_2 r)}{\mu_2 r} .$$

The parameters given by Satchler and Love, namely $U_1 = 6315$ MeV, $\mu_1 = 4$ fm$^{-1}$, $U_2 = -1961$ MeV and $\mu_2 = 2.5$ fm$^{-1}$ produce a potential which is, as noted by the authors, slightly too small in the tail. The best fit is obtained by varying slightly the strength $U_2$ of the second Yukawa potential from -1961 MeV to -2264 MeV or its range $\mu_2$ from 2.5 fm$^{-1}$ to 2.42 fm$^{-1}$. In both cases the fit to the data is exactly as good as with standard Woods-Saxon potential, such as shown in Figs. 11 and 12. This interaction, with $\mu_2 = 2.42$ fm$^{-1}$, was then folded into the Hartree-Fock density of $^{16}O$ in order to produce a nucleon-$^{16}O$ effective interaction with which we will now proceed to analyse (a) which region of the nucleon density of $^{40}Ca$ is most sensitive to the data and (b) other isotopes. This effective nucleon-$^{16}O$ force is shown in Fig. 14 (full curve). On the same figure are plotted two approximations to it, which give in practice identical results, namely a Woods-Saxon form (dashed line, open circles)

$$\frac{22.45}{1 + \exp \frac{r-3.70}{0.51}} \quad \text{(MeV, r in fm)}$$

and a gaussian form (dotted line, open triangles)

$$137 \exp(-(0.42\, r)^2) \text{(MeV, r in fm)}.$$

Which is the radial region of the $^{40}Ca$ density which is most sensitive to $^{16}O$ scattering data near the Coulomb barrier? In order to answer this question let us first consider the following Fermi-2 parameter parameterization of the Hartree-Fock density of $^{40}Ca$ :

$$\rho(r) = \frac{0.1345}{1 + \exp \frac{r-3.88}{0.452}}.$$

This distribution differs from the Hartree-Fock one in the interior of the nucleus, but is within 1-2 % of it for r > 4 fm. It gives an equally good fit to the data. The diffuseness parameter of this distribution was varied from 0.400 to 0.575 fm in steps of 0.025 fm. In all cases an equally good fit could be obtained. All such densities fall in the hatched region of Fig. 15 where the Hartree-Fock density of Campi [15] is represented by a full line. It appears

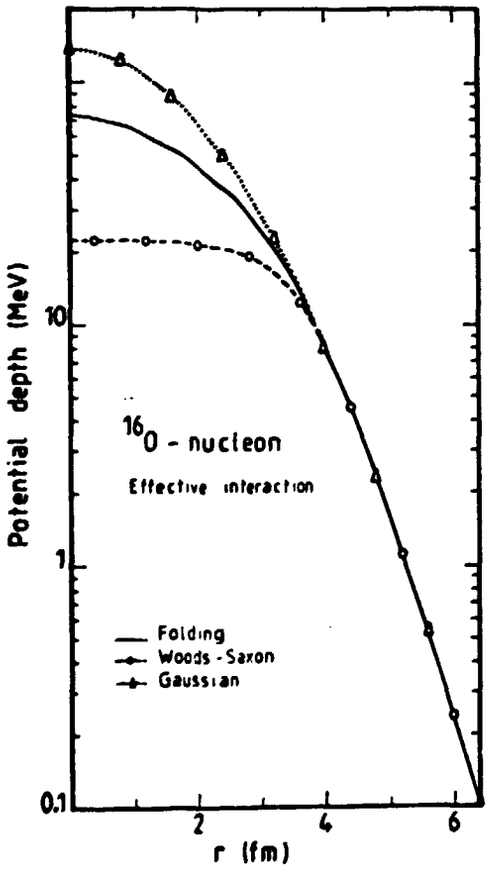


*Figure 14*

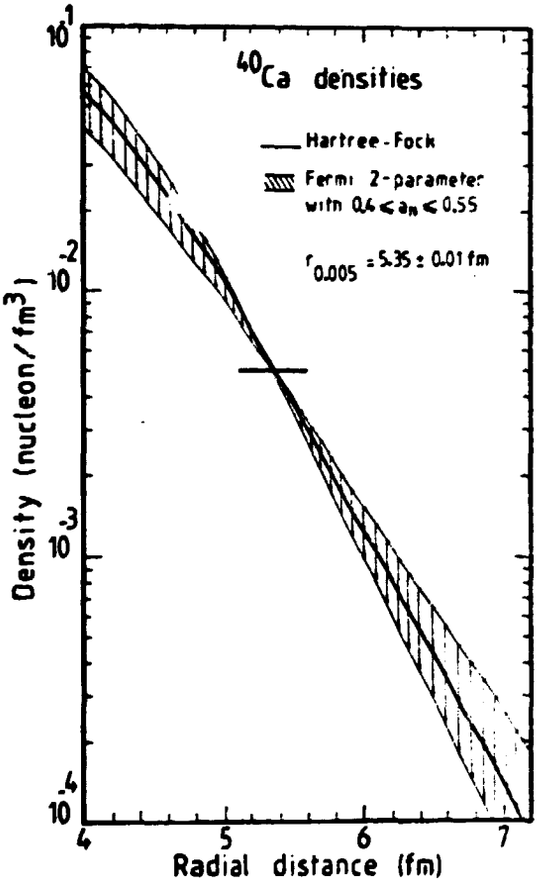


*Figure 15*

that all distributions cross in a radial region where the density is about $5 \times 10^{-3}$ nucleon/fm$^3$, and in turn the elastic scattering of $^{16}O$ from $^{40}Ca$ is mainly influenced by a size parameter which can be taken as the radial distance $r_{0.005}$ where the $^{40}Ca$ density is $5 \times 10^{-3}$ nucleon/fm$^3$. For $^{40}Ca$, $r_{0.005} = 5.35$ fm.

The potentials generated by these density distributions are shown in the upper part of Fig. 13. They all cross for a depth of about 1 MeV, and give

$$R_{1.0} = 9.53 \pm 0.01 \text{ fm} \quad \text{or} \quad R_{0.8} = 9.65 \pm 0.02 \text{ fm}$$

in agreement with the value deduced from the Woods-Saxon analysis, but rather on the high side.

The same analysis was then performed on the $^{48}Ca$ data, using the same nucleon-$^{16}O$ interaction. Very similar results are obtained, namely :

i) all potentials which give a good fit to the data cross in a region where they are about 1-MeV deep, and for $^{48}Ca$, $R_{0.8} = 9.84 \pm 0.01$ fm,

ii) all densities (of Fermi shape) which give a good fit to the data give $5 \times 10^{-3}$ nucleon/fm$^3$ at the same distance $r_{0.005} = 5.54 \pm 0.01$ fm.

From the $^{40}Ca$ and $^{48}Ca$ analyses, it is now possible to deduce the following simple relationship for this region :

$$r_{0.005} = R_{0.8}^{(WS)} - 4.30 \pm 0.02 \text{ fm.}$$

This relationship enables one to deduce $r_{0.005}$ from a simple Woods-Saxon analysis. Values of $r_{0.005}$ were in particular deduced that way from the results of ref.[12]. All results are summarized in table 1.

Table 1

| Isotope | Ref. | $R_{0.8}$ | $r_{0.005}$ | |
|---|---|---|---|---|
| | | | exp. | theory [15] |
| $^{40}Ca$ | 13 | 9.65 | 5.35* | 5.35* |
| $^{40}Ca$ | 12 | 9.58 | 5.28 | |
| $^{44}Ca$ | 12 | 9.70 | 5.40 | |
| $^{48}Ca$ | 13 | 9.84 | 5.54 | 5.58 |
| $^{48}Ca$ | 12 | 9.88 | 5.58 | |

* taken as reference

There are some discrepancies between the data of refs.[12] and [13], which are not explained. The difference between $r_{0.005}$ values for $^{40}Ca$ - $^{48}Ca$ are 0.19 fm for ref.[13] and 0.30 fm for ref.[12] while the Hartree-Fock calculation gives 0.23 fm. It is hard to decide at present if such a discrepancy can be attributed to standard experimental uncertainties, or to some systematic difference in the data or in the analysis. Such a discrepancy was already apparent

in the analysis of Groeneveld et al.[13].

## Summary

The elastic scattering of strongly absorbed particles near the Coulomb barrier is sensitive to one size parameter, which is the distance at which the real nuclear potential has some fixed value, 0.2 MeV for α-particle, 1 MeV for $^{16}O$. This size parameter can be related in a simple way to the radial distance of the target nucleus where the density takes some given value, $2 \times 10^{-3}$ nucleon/fm$^3$ for α-particle scattering and $5 \times 10^{-3}$ nucleon/fm$^3$ for $^{16}O$ scattering.

## References


[1] I. Badawy, B. Berthier, P. Charles, M. Dost, B. Fernandez, J. Gastebois and S.M. Lee, Phys. Rev. C17, 978 (1978).

[2] A.R. Barnett and J.S. Lilley, Phys. Rev. C9, 2010 (1974).

[3] S.L. Tabor, B.A. Watson and S.S. Hansen, Phys. Rev. C11, 198 (1975).

[4] D.F. Jackson and M. Rhoades-Brown, Nucl. Phys. A266, 61 (1976).

[5] G. Goldring, M. Samuel, B.A. Watson, M.C. Bertin and S.L. Tabor, Phys. Lett. 32B, 465 (1970).

[6] P. Mailandt, J.S. Lilley and G.W. Greenlees, Phys. Rev. Lett. 28, 1075 (1972) ; Phys. Rev. C8, 2189 (1973).

[7] J. Heisenberg, R. Hofstadter, J.S. McCarthy, I. Sick, B.C. Clark, R. Herman and D.G. Ravenhall, Phys. Rev. Lett. 23, 1402 (1969).

[8] W.Q. Sumner, Ph.D. Thesis, University of Washington, 1974 (unpublished) ; W.Q. Sumner and J.S. Blair, to be published.

[9] J.W. Negele, Phys. Rev. C1, 1270 (1970).

[10] C.J. Batty, E. Friedman and J.F. Jackson, Nucl. Phys. A175, 1 (1971).

[11] A.M. Bernstein, Advan. Nucl. Phys. 3, 325 (1969).

[12] M.C. Bertin, S.L. Tabor, B.A. Watson, Y. Eisen and G. Goldring, Nucl. Phys. A167, 216 (1971).

[13] K.O. Groeneveld, L. Meyer-Schützmeister, A. Richter and U. Strohbusch, Phys. Rev. C6, 805 (1972).

[14] R.A. Chatwin, J.S. Eck, A. Richter and D. Robson, in "Nuclear physics induced by heavy ions", edited by R. Bock and W. Hering (North Holland, Amsterdam, 1970) p. 76.

[15] X. Campi and D.W. Sprung, Nucl. Phys. A194, 401 (1972).

[16] G.R. Satchler and W.G. Love, Phys. Lett. 65B, 415 (1976).